



HAL
open science

2D vertical field-effect transistor

Daniela Di Felice, Yannick J. Dappe

► **To cite this version:**

Daniela Di Felice, Yannick J. Dappe. 2D vertical field-effect transistor. *Nanotechnology*, 2018, 29, pp.505708. 10.1088/1361-6528/aae406 . cea-01936725

HAL Id: cea-01936725

<https://cea.hal.science/cea-01936725>

Submitted on 27 Nov 2018

HAL is a multi-disciplinary open access archive for the deposit and dissemination of scientific research documents, whether they are published or not. The documents may come from teaching and research institutions in France or abroad, or from public or private research centers.

L'archive ouverte pluridisciplinaire **HAL**, est destinée au dépôt et à la diffusion de documents scientifiques de niveau recherche, publiés ou non, émanant des établissements d'enseignement et de recherche français ou étrangers, des laboratoires publics ou privés.

PAPER

2D vertical field-effect transistor

To cite this article: D Di Felice and Y J Dappe 2018 *Nanotechnology* **29** 505708

View the [article online](#) for updates and enhancements.



IOP | ebooks™

Bringing you innovative digital publishing with leading voices to create your essential collection of books in STEM research.

Start exploring the [collection](#) - download the first chapter of every title for free.

2D vertical field-effect transistor

D Di Felice and Y J Dappe¹ 

Service de Physique de l'Etat Condensé, DSM/IRAMIS/SPEC, CNRS UMR 3680, CEA Saclay, Université Paris-Saclay, F-91191 Gif-Sur-Yvette, France

E-mail: yannick.dappe@cea.fr

Received 23 July 2018, revised 18 September 2018

Accepted for publication 25 September 2018

Published 17 October 2018



CrossMark

Abstract

Within the framework of 2D materials, we present four theoretical models of a vertical field-effect transistor (FET) composed of simple alternate graphene and MoS₂ layers. The electronic transport properties at a specific graphene/MoS₂ interface in each configuration are investigated by focusing in particular on the current as a function of the gate voltage. The gate voltage, simulated with a shift of the bands of a specific layer, allows us to tune the current at the interface and the charge transfer between the planes. This analysis of the charge transfer as a function of the gate voltage reveals a strong connection with the transport characteristics as the slope of the current curve. The analysis of physical phenomena at the graphene/MoS₂ interface can further improve the 2D vertical FET performance and contribute to the development of new 2D nanotechnology.

Keywords: graphene and 2D materials, density functional theory, electronic transport, transistor

(Some figures may appear in colour only in the online journal)

1. Introduction

The field-effect transistor (FET) is an electronic device representing the basic building block of modern technology based on semiconductor electronics. It consists of an electronic device used to amplify or switch the current, composed of a semiconductor channel connected with two metallic contacts, where the flowing current can be tuned by applying an electric field. Generally speaking, the progress of information and communication technology comes from the effort in improving the performances of this electronic component [1]. Traditionally, FETs are based on bulk or 3D semiconductor channels composed of silicon, and GaAs and GaN semiconductors. Following Moore's law, which in 1965 predicted that the density of transistors in a chip will double every two years [2–5], the 3D materials have been scaled down to nanoscale dimension over the past five decades. Of course, there is a limit to the size reduction of 3D FETs related to short-channel [6, 7] and surface effects, due to dangling bonds, which cause the deterioration of transistor performance. After the discovery of graphene [8, 9], many other graphene-like materials such as germanene, silicene and transition metal dichalcogenides started to be included in electronic devices to overcome some of the previously cited undesired effects.

Many 2D FETs, mostly based on graphene due to its extraordinary properties, have been built or theoretically modeled in recent years. However, graphene does not present any gap, which is strictly necessary in electronics. One way to overcome this problem is to combine graphene with a 2D semiconductor such as MoS₂ in a van der Waals (vdW) heterostructure, a vertical stacking of different 2D materials able to keep the main characteristics of each material [10]. In an FET architecture, the 2D materials can play the role of an in-plane channel [11, 12] or barrier [13–16]. In principle, for a tunneling transistor such as that proposed by Britnell *et al.*, graphene is used because of the low density of states (DOS), responsible for the greater increase of E_F with respect to conventional 2D gas with parabolic dispersion, as a gate voltage is applied [17–21]. However, the absence of a band gap in graphene affects the performance of the transistor, due to the low ON/OFF ratio. Recently, an FET fully composed of 2D materials was built with graphene contacts, hBN dielectric and MoS₂ channel, exhibiting good performance [22].

In this work, we present a very simple model for FET bases on the interface graphene-MoS₂ monolayer, where the two monolayers are used as the source-drain electrodes. The MoS₂ monolayer is included because of its band gap, used to switch ON/OFF the device. By means of density functional theory (DFT) and non-equilibrium Green's function formalism, we are able to simulate the effect of the gate voltage and calculate the transverse current between the graphene and

¹ Author to whom any correspondence should be addressed.

MoS₂. Despite the used approximations and its simplicity, this model is able to reproduce the transistor operations, allowing the complete investigation of the electronic transport at the graphene-MoS₂ interface. In particular, we focus on the modification of the transport current, modulated by the gate voltage, between the electrodes when additional alternate layers of graphene and MoS₂ are stacked on top of them.

Then, a mixed heterostructure (hBN/graphene/MoS₂) and the interface graphene/hBN are also presented to demonstrate the independence of the interfaces and the role of the band edge shape in the transport parameters. We believe that this kind of study is necessary to define the possible role of the vertical vdW heterostructures in the new FET generation.

2. Method of calculation

All the results we present in this work have been obtained within DFT methodology. Both the self-consistency and transport calculations are performed within the Fireball code, a very efficient DFT-localized orbital method [23, 24]. This code uses a self-consistent version of the Harris–Foulkes local density approximation (LDA) functional [25, 26] and the self-consistency is achieved over the occupation numbers. The unit cell optimization and inclusion of the vdW interaction using the LCAO-S² + vdW approach are presented in detail in appendix A.

Then, using the Hamiltonian calculated within the Fireball methodology, the electronic current can be estimated following the non-equilibrium Green's function technique developed by Keldysh [27]. The complete system can be virtually separated for the current calculation into two subsystems (even though the whole system is fully diagonalized in Fireball) given by the different layers and labeled T and S. These two parts are joined in the current equation through a mutual interaction (T_{TS} and T_{ST} , which correspond to the hopping integrals calculated in the Fireball code).

$$I = \frac{4\pi e^2}{h} \int_{E_F}^{E_F+eV} \text{Tr}[T_{TS} \rho_{SS}(\omega) D_{SS}^r(\omega) T_{ST} \rho_{TT}(\omega - eV) \times D_{TT}^a(\omega - eV)] d\omega, \quad (1)$$

where ρ_{TT} and ρ_{SS} are the density matrices of the two subsystem, respectively; $D_{TT}^a = \{\hat{I} - \hat{T}_{ST} \hat{g}_{TT}^a(\omega) \hat{T}_{TS} \hat{g}_{SS}^a(\omega)\}^{-1}$ and $D_{SS}^r = \{\hat{I} - \hat{T}_{ST} \hat{g}_{TT}^r(\omega) \hat{T}_{TS} \hat{g}_{SS}^r(\omega)\}^{-1}$ matrices are related to the multiple scattering effect produced by potential electronic reflections that could occur when the two subsystems are close to each other. The two terms $\hat{g}_{SS/TT}^{r/a}$ are the Green's function for the non-interacting case. The final equation is obtained at 0 K temperature and a bias voltage V . A complete description of the methodology can be found in [28].

To simulate the gate voltage and effect of the band shifting, we used a scissor operator [29, 30] described in appendix B, able to move each band $\varepsilon_\alpha(\mathbf{k})$ a value $\Delta_\alpha(\mathbf{k})$.

In this work, we consider four different stacking configurations based on MoS₂ and graphene planes. Since

graphene and MoS₂ have different lattice parameters, it is necessary to build a supercell commensurate with both MoS₂ and graphene. In particular, our bricks to build the four supercells are composed of four MoS₂ and seven graphene unit cells mutually rotated by 15 degrees. Due to the periodic boundary conditions and the mismatch of the lattice parameters, a strain on graphene is present, since we keep the MoS₂ in its optimized configuration. In fact, the strain on graphene does not affect the electronic and transport properties, unlike what happens in strained MoS₂. As we demonstrated in a previous work [31], the orientation between the layers in a heterostructure where the interlayer force is the weak vdW interaction, does not affect the global electronic properties. This suggests that any oriented supercell is equivalent from the global transport point of view. Hence, we will use the smallest possible unit cell in order to reduce the calculation time, since we know that the orientation between the layers does not affect the electronic transport properties of the interface.

3. Results

In this model, the main idea is to combine the gap of MoS₂ with the graphene characteristics, using these two 2D crystals as electrodes. The transverse current between graphene and the MoS₂ electrodes, I_{SD} , is allowed by the voltage applied between the two layers, called the source-drain voltage V_{SD} , and it can be tuned or switched by means of a second voltage V_G , able to modify the band alignment between the two planes. The gate voltage V_G is responsible for the shift of the bands of graphene with respect to the gap of MoS₂, simulated by applying the scissor operator on it, which represents the effective gate potential felt by graphene (normally reduced by ~ 100 times with respect to the real applied gate potential when a dielectric of 300 nm of SiO₂ is placed between the gate and the electrode).

The transverse current I_{SD} occurs only if there are accessible states on both electrodes. In graphene, there are always available electrons (except at the Dirac point) for the current, whereas in MoS₂, due to the gap, the current is possible only if we fall into the conductance band (CB) or valence band (VB). For a specific range of V_G corresponding to the gap value, the band alignment is such that the Fermi level falls in the gap of MoS₂ and the current is forbidden; out of this range, the Fermi level approaches the CB (or VB) and the device switches to the ON state. The Fermi level on the VB and CB leads to a charge transfer (Q) between graphene and MoS₂, or in other words to a charge redistribution between the planes, that is found to be at the basis of the device operation.

In the following, we will first analyze the characteristics of the simple graphene/MoS₂ heterostructure as a transistor and then we stack additional layers forming further systems as graphene/MoS₂/graphene with V_G applied on the first graphene and on both, and graphene/MoS₂/graphene/MoS₂.

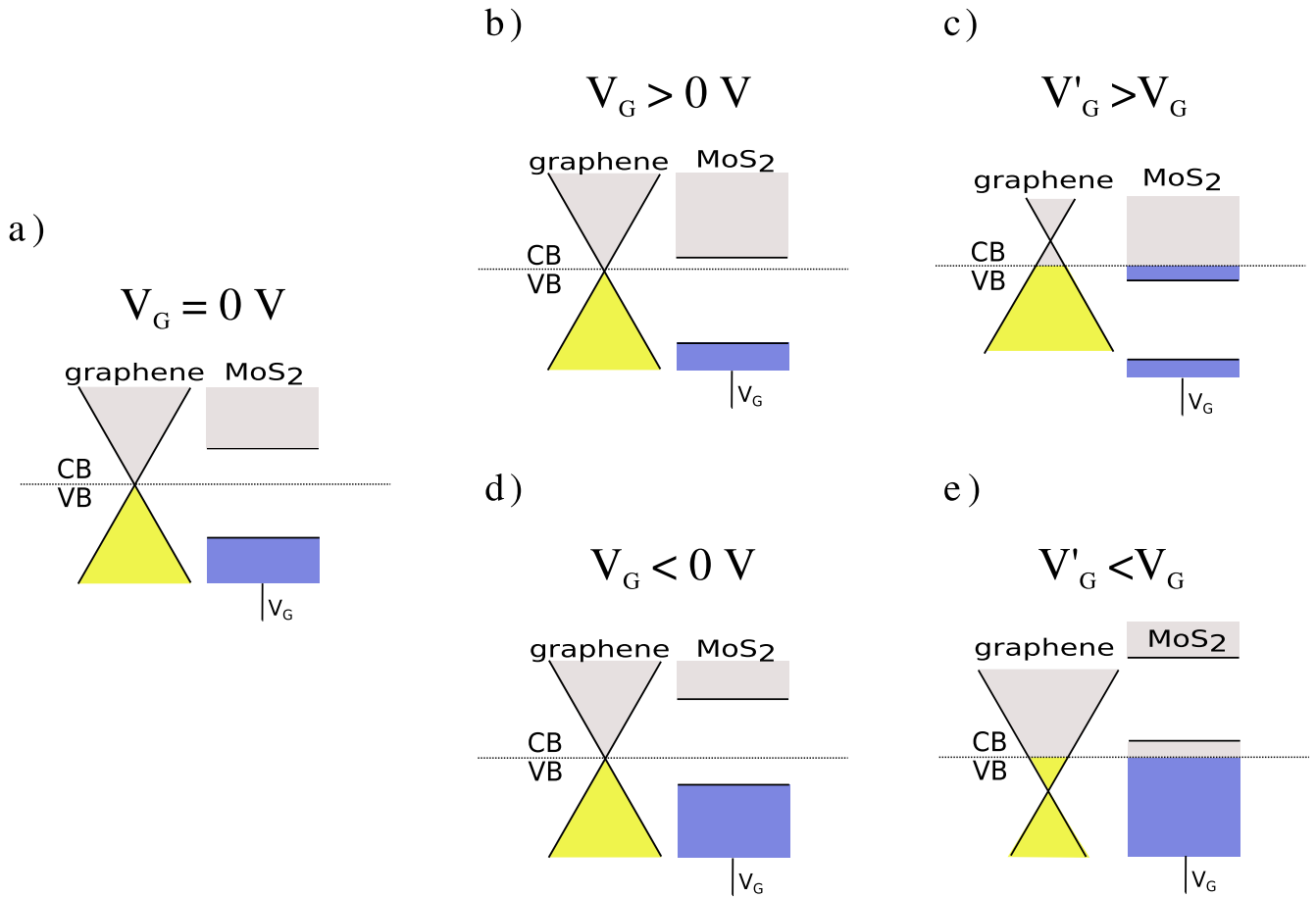


Figure 1. Band diagrams: alignment of graphene and MoS₂ Fermi electronic levels for positive and negative V_G , where the Dirac cone falls in the MoS₂ gap (panel b and c) and for larger absolute values where the Dirac cone falls in the CB and VB, in panel d) and e), respectively.

3.1. Band alignment in graphene/MoS₂ heterostructure

We start by describing the effects of the band alignment in the graphene/MoS₂ interface shown in figure 1. Starting from the initial position, namely for $V_G = 0$ V, the Dirac point falls in the MoS₂ gap (at -0.6 V from the CB), and moves towards the CB as the voltage positively increases, or towards the VB when V_G is negative. For positive gate voltages, the graphene bands shift to higher values; the Fermi level defined by graphene moving towards the CB, as can be seen in figure 1(b). For more positive voltages, the Fermi level moves on the CB and a migration of electrons from graphene to MoS₂ occurs (see figure 1(c)), providing the accessible states for the current.

In the case of negative V_G , we have an opposite shift and the migration of electrons from MoS₂ to graphene occurs when the Fermi level falls on the VB (compare figures 1(c) and (e)). In the following sections, we will refer to this migration of electrons from graphene to MoS₂ as the charge transfer Q on MoS₂ and vice versa.

In order to understand the mechanism of our transistor, it is necessary to take a look at the band shift, by means of the DOS alignment for different V_G . First of all, we observe that the shift of the graphene DOS with respect to the MoS₂ DOS as a function of V_G is not linear, but depends on the position of the Fermi level (falling almost in correspondence with the

Dirac point), with respect to the MoS₂ gap, to the CB and VB. Hence, when the Fermi level falls in the MoS₂ gap, an increase of the gate voltage of 1 V (from 0 to +1.0 V in figures 2(b) and (c)) yields a shift of the band structure of almost 0.7 eV. On the other hand, when the Fermi level approaches the CB (or VB), the same V_G increased by 1 V, which causes a reduced shift of the DOS, since a charge transfer from graphene to MoS₂ (or from MoS₂ to graphene) occurs, oppositely to the applied gate. This reaction of the system to the applied band shift on graphene is discussed in appendix B.

This means that, in order to reach the first electronic states in CB (VB) of MoS₂, and consequently the current saturation, we need an effective V_G , which is larger than the value of the gap. This is the reason we need to calculate the electric current for a range of V_G from -5 to $+5$ V (larger than the gap of MoS₂). Note that when the Dirac point is in the gap, it defines the Fermi level, whereas when it is close to CB (VB), the charge transfer from graphene to MoS₂ (from MoS₂ to graphene) results in an electronic doping of graphene causing a displacement of the Fermi level from the Dirac point.

3.2. Graphene/MoS₂ electronic transport properties

We now move to the quantitative evaluation of the charge transfer for graphene/MoS₂ by plotting the $Q(V_G)$ curve

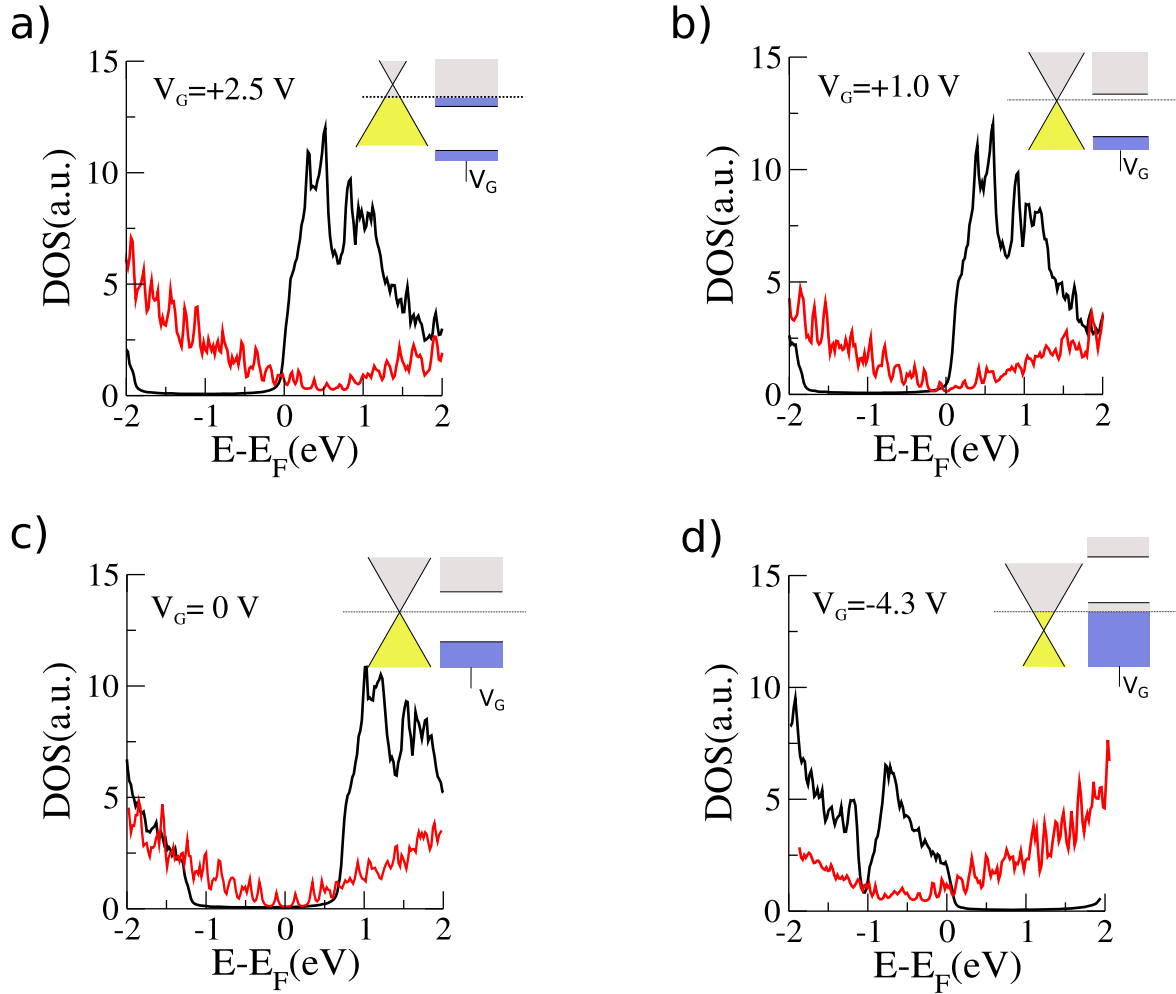


Figure 2. DOS and the relative band alignment for different values of V_G . Red (black) line corresponds to graphene (MoS₂) DOS. Graphene DOS has been multiplied by five, in order to directly compare the two DOS.

(see figure 3(a) for the structure). As previously mentioned, the approach of the Fermi level to CB or VB leads to a charge transfer Q between the layers. In figure 3(c), we plot Q at the interface as a function of V_G . This curve shows three regions characterized by linear behavior with two different slopes. The plateau-like part (with smaller slope) coincides with the Fermi level moving in the MoS₂ gap, namely for a range of V_G of ~ 2 V, corresponding to the OFF state of the transistor (here we can still find finite $Q = 0.18$ e/unit cell, even for $V_G = 0$ V, coming from the interaction between the layers). Then, right out of the OFF range of V_G , we found the very important part, we call the switch region, defined as the range of V_G where the Q curve changes its slope from the OFF to the ON linear parts, occupying around 1 V in this case; the change of slope does not suddenly occur. For larger V_G , we recover the two second linear regions, for positive and negative voltages. We note that even in the OFF region, we have a charge transfer Q that leads to a non-zero electronic density in the gap of MoS₂.

In figure 3(b), we show the behavior of $I_{SD}(V_{SD})$ calculated for a range of V_{SD} between -0.5 and $+0.5$ V and for different V_G . For gate voltage $V_G = -1.0$ V, corresponding to the OFF state of the transistor, the current is very low.

However, when the Dirac cone approaches the VB (CB), for $V_G < -1.7$ V ($V_G > +0.3$ V), we observe an increase of the positive (negative) branch of the current curve for positive (negative) V_{SD} ; this corresponds to the ON state.

In figure 3(d), the current $I_{SD}(V_G)$ for $V_{SD} = -0.1$ V is shown for a V_G range between -5 and $+6$ V, corresponding to the range where the ON/OFF switch occurs. Again, in the OFF region around -1.5 and $+0.5$ V, we found very low current corresponding to the plateau in $Q(V_G)$, whereas in the ON region we can find two important parts: one is the increase of $I_{SD}(V_G)$, related to the change of Q slope, and the other one is the saturation of the current, for $V_G > 2.0$ V and $V_G < -3.0$ V, corresponding to the second linear region of Q . The main parameters we want to modify by stacking an additional layer is the slope of $I_{SD}(V_G)$ and the ratio between the higher and lower current, called the ON/OFF ratio, which defines how good the performance of the transistor is.

In this work, the slope of $I_{SD}(V_G)$ is defined as the increase of the current curve in the V_G range from 0 to $+2$ V, whereas the ON/OFF ratio is the ratio between the current at $V_G = 5$ V and the current at $V_G = 0$ V. In this first configuration, we found a slope of $\sim 2 \times 10^2$ and an ON/OFF ratio of $\sim 2.4 \times 10^2$.

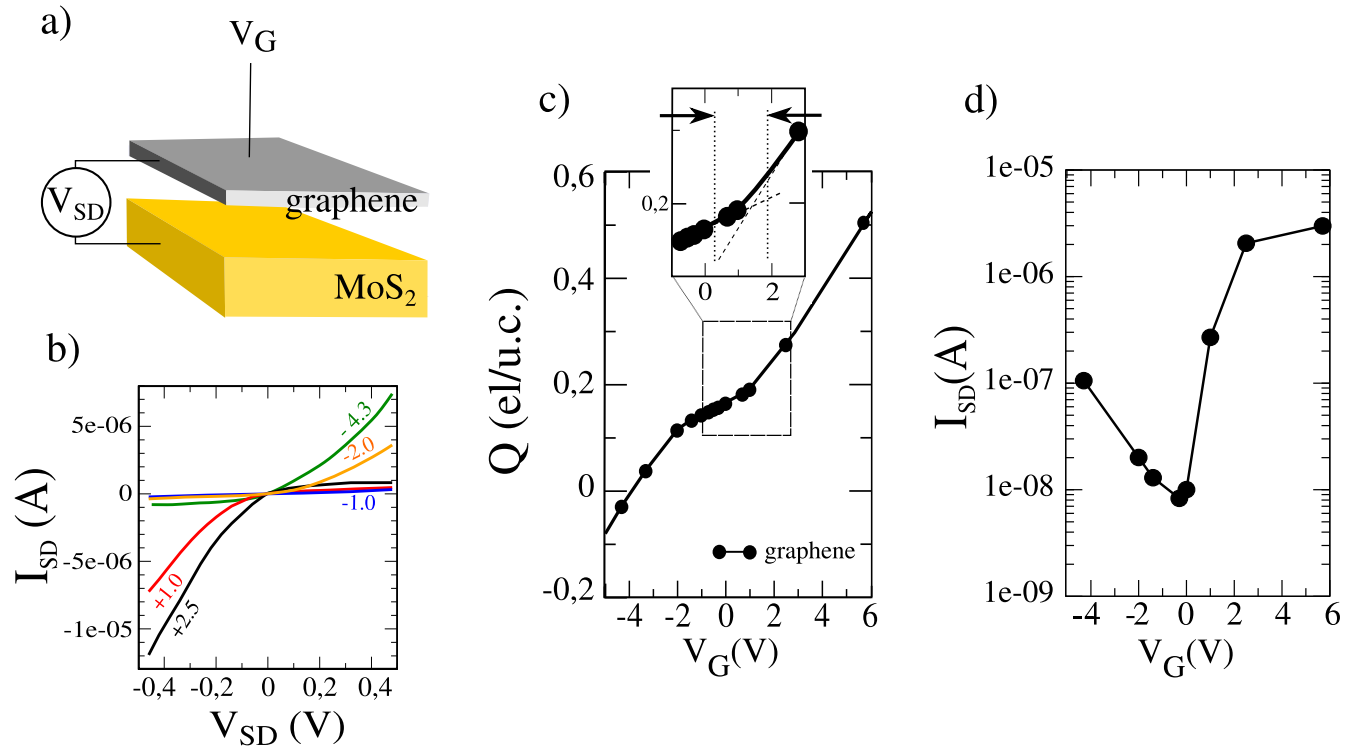


Figure 3. Graphic representation of the transistor model composed of graphene/MoS₂ heterostructure is illustrated in (a), the current $I_{SD}(V_{SD})$ for different V_G in (b). Charge transfer with a zoom on the switch region and the current as a function of the gate voltage $I_{SD}(V_G)$ for $V_{SD} = -0.1$ V are shown in (c) and (d), respectively.

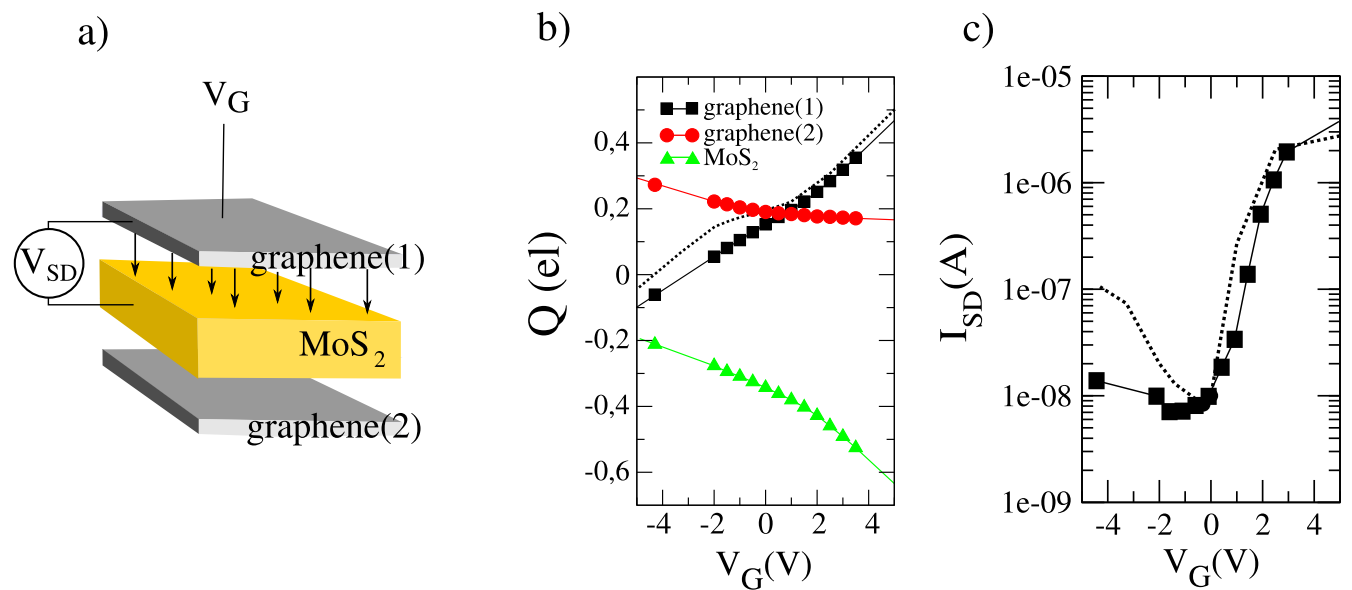


Figure 4. Graphic representation of the transistor model composed of graphene(1)/MoS₂/graphene(2) heterostructure in (a), charge transfer Q on graphene(1), graphene(2) and MoS₂ in black, red and green, respectively, are plotted in (b). In (c), $I_{SD}(V_G)$ for $V_{SD} = -0.1$ V is shown together with the current obtained in the first case, in a solid and dashed line, respectively.

3.3. Graphene/MoS₂/graphene heterostructure

Starting from graphene/MoS₂ heterostructure, we now stack an additional graphene, obtaining graphene(1)/MoS₂/graphene(2) where, as previously, graphene(1) and MoS₂ are the source and drain electrodes (see figure 4(a)).

As is known from the previous work [31], the presence of the second graphene does not affect the electronic properties of the component layers. However, its presence modifies the band alignment, strictly connected to the charge transfer Q , and then to the current. In figure 4(b), we plot Q for each

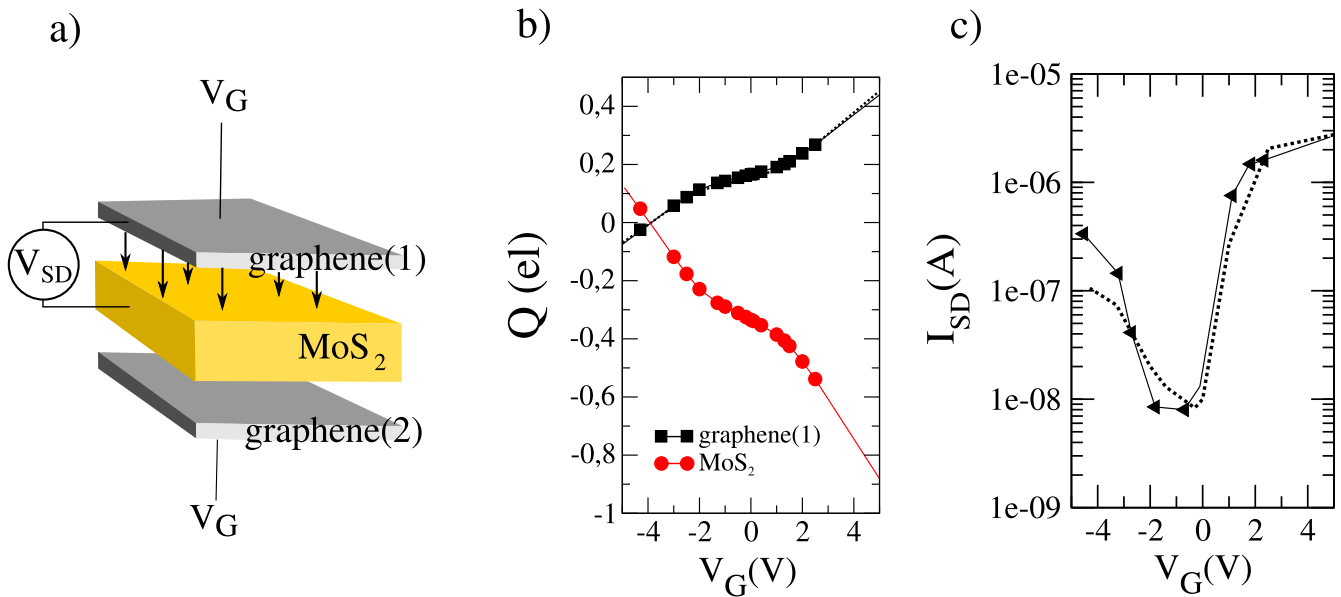


Figure 5. Graphic representation of the transistor model composed of graphene(1)/MoS₂/graphene(2) with V_G applied on both graphenes in (a) and charge transfer Q on graphene and MoS₂ (black and red line, respectively) is shown in (b). In (c), $I_{SD}(V_G)$ for $V_{SD} = -0.1$ V is shown together with the current obtained in the first case, in a solid and dashed line, respectively.

layer, in black, red and green lines for graphene(1), MoS₂ and graphene(2), respectively. The dashed lines correspond to the charge transfer on graphene in the original graphene/MoS₂ heterostructure. We found that the charge transfer for all three layers is very different from what we had before. The first difference is that Q varies less with respect to V_G than in the previous graphene/MoS₂ device, due to the presence of the second graphene layer. Furthermore, here, we do not have the three linear regions as before and Q on graphene(1) has almost the same slope for the whole V_G range. Looking at Q on MoS₂, however, we can recognize two regions from -5 to $+0.5$ V and from $+0.5$ to $+5.0$ V, characterized by small and very smooth change of slope.

The transverse current calculated at the graphene(1)-MoS₂ interface, $I_{SD}(V_G)$, is represented in figure 4(c). The change of Q is reflected in the current behavior: the OFF region seems to be larger, according to the absence of the third linear region in Q for negative V_G , and also for positive values, the increase of I_{SD} is slower than in the previous transistor, as Q increases slowly. The absence of the change of the switch region for negative V_G is reflected in the low current.

In this configuration, the presence of the second graphene layer reduces the effect of V_G in the switching of the charge transfer curve from the OFF to the ON region. In fact, the switch region increases and, consequently, the current shows a smoother increase with respect to graphene/MoS₂, clearly visible since here it is necessary to apply a larger value of V_G of 1 V to recover the same current as in the previous graphene/MoS₂ system. This results in a worsening of the transistor parameter given by the slope of I_{SD} ($\sim 1.4 \times 10^2$). However, the ratio between the larger and the lower current appears to be larger than in the previous case, being almost 10^3 . The idea is to try to increase the velocity of the band

shift, which can be analyzed by looking at the Q shape, in particular at the switch between the linear regions, which should be as small as possible to lead to a faster increase of I_{SD} . In other words, we want the Fermi level to move as fast as possible towards the CB or VB edges of MoS₂. We will try to achieve this by using the heterostructure and by applying the gate voltage on the two graphene layers.

3.4. Double gate on the two graphene layers

By considering the same heterostructure graphene(1)/MoS₂/graphene(2) (figure 5), it is possible to make something different; we apply the same gate voltage in both graphene layers in order to also use the second graphene as an active component, by also shifting its band. This is a symmetric system from the point of view of the band shift, composed by two distinct and equivalent interfaces: graphene(1)-MoS₂ and MoS₂-graphene(2), being the first interface where the V_{SD} is applied and the current calculated.

The symmetric configuration ensures that both graphene layers present the same alignment. The analysis of the charge transfer and the transport characteristics have been repeated in this new configuration and the results are presented in figure 5.

First of all, we take a look at the charge transfer. Obviously, we find the same Q curve on both graphene layers, as we expected from the symmetry of the system. Then, we note that the Q curve corresponds to the one found on graphene in the first configuration (compare the black continuous and dashed lines in figure 5(b)), revealing a kind of independence between the two graphene(1)/MoS₂ and MoS₂/graphene(2) interfaces.

Here, the same V_G brings about doubled charge transfer on the MoS₂ electrode with respect to the original

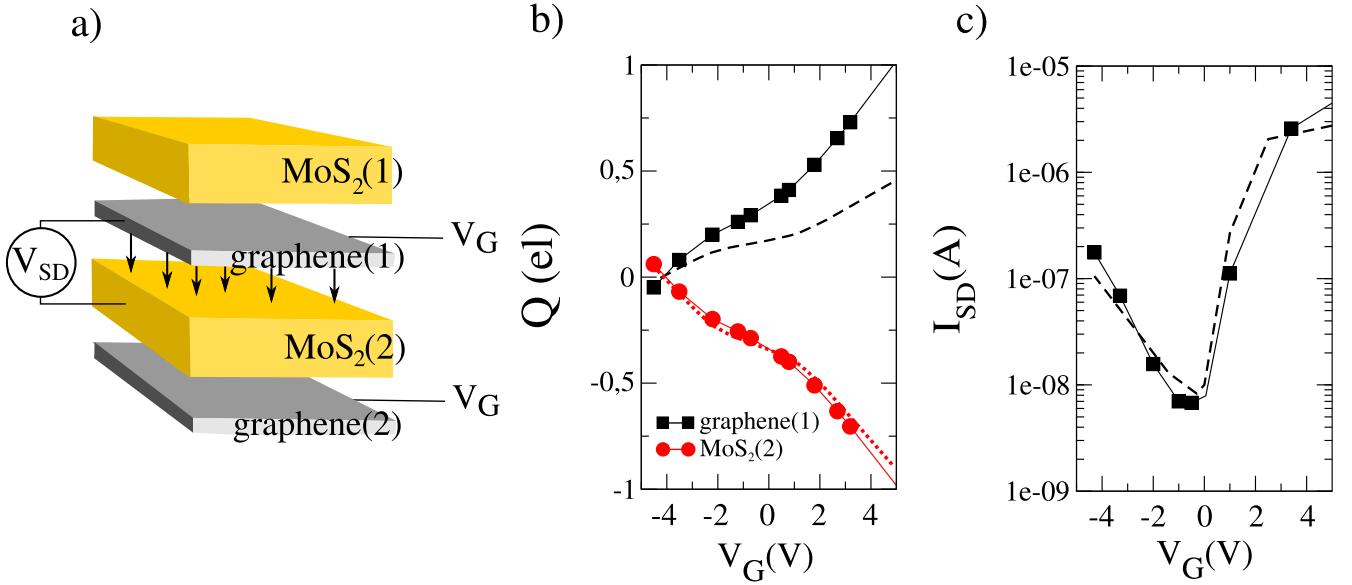


Figure 6. Graphic representation of the transistor model composed of MoS₂(1)/graphene(1)/MoS₂(2)/graphene(2) is shown in (a); the charge transfer Q on graphene(1) and MoS₂(2) (black and red line, respectively) is compared with the charge transfer obtained in the graphene/MoS₂ case (dashed lines) with the scissor on graphene in (b). In (c), $I_{SD}(V_G)$ for $V_{SD} = -0.1$ V is shown together with the current obtained in the first case, in the solid and dashed line, respectively.

graphene/MoS₂ interface, in both ON and OFF zones. However, the switch region is not thinner than in the previous case, which means that the same range of V_G as in MoS₂/graphene is necessary to move from the OFF to the ON part. The consequence is that the increase of the current does not occur faster than before. Consequently, we do not expect a significant improvement of I_{SD} with respect to the graphene/MoS₂ interface, as can be observed when comparing the continuous and dashed lines in figure 5(c). We also note that, as a consequence of the Q doubling on the OFF and ON region, the ratio between the two slopes of the Q curve calculated on MoS₂ characterizing the ON and OFF regions does not change.

3.5. MoS₂/graphene/MoS₂/graphene heterostructure

Considering the results of the previous cases, we now move to the last configuration: MoS₂(1)/graphene(1)/MoS₂(2)/graphene(2) heterostructure with gate voltage applied on two graphene planes (figure 6(a)). The electrodes are graphene(1) and MoS₂(2).

Following our idea, we expect to find twice the amount of charge transfer Q on both electrodes, as can be seen in figure 6(b), where Q on graphene (black line) and Q on the MoS₂ electrodes are shown and compared to the charge transfer in the simple graphene/MoS₂ configuration (dashed line). We confirm that the charge transfer between the layers can be evaluated by considering each interface independently from the others.

Also, in this latter case, we can relate the charge transfer (figure 6(b)) and I_{SD} (figure 6(c)). We found that the slope of

the current is not improved with the additional MoS₂ and graphene layers, whereas we can find a larger ON/OFF ratio.

3.6. hBN/graphene, the charge transfer depends on the DOS

At this point, after a complete description of the role of the additional layers in the electronic transport characteristics, we want to focus on the intrinsic parameters affecting the slope of $I_{SD}(V_G)$. We show here that the fundamental role is played by the shape of the DOS in the CB and VB edges. The way the DOS increases, since we do not have a perfect sharp band edge, is reflected on the charge transfer curve, in the switch region and then in the current slope. In the end, the slope ratio between the OFF and ON Q region is a consequence of the DOS shape at the gap edges.

A simple test is performed on the hBN/graphene heterostructure shown in figure 7(a). The hBN is not suitable as an electrode because of its very large band gap. However, it provides a very clear example to demonstrate how the shape of the CB and VB edges affects the increase of the current.

The switch of the charge transfer from the OFF to the ON linear region of hBN/graphene and graphene/MoS₂ (blue and red lines in figure 7(b), respectively) is stressed by the arrows in the zoom on the right. In hBN/graphene the change of slope from the OFF to the ON region occurs at ~ 5 V, whereas for MoS₂/graphene it occurs at less than 2 V; this provides a larger switch region for hBN/graphene. Thus, we expect a smoother increase of the I_{SD} curve compared to the current in graphene/MoS₂, as shown by the blue and the red lines, respectively, in figure 7(c).

The very slow increase of the charge and, consequently, of the current with respect to the graphene/MoS₂ case, is

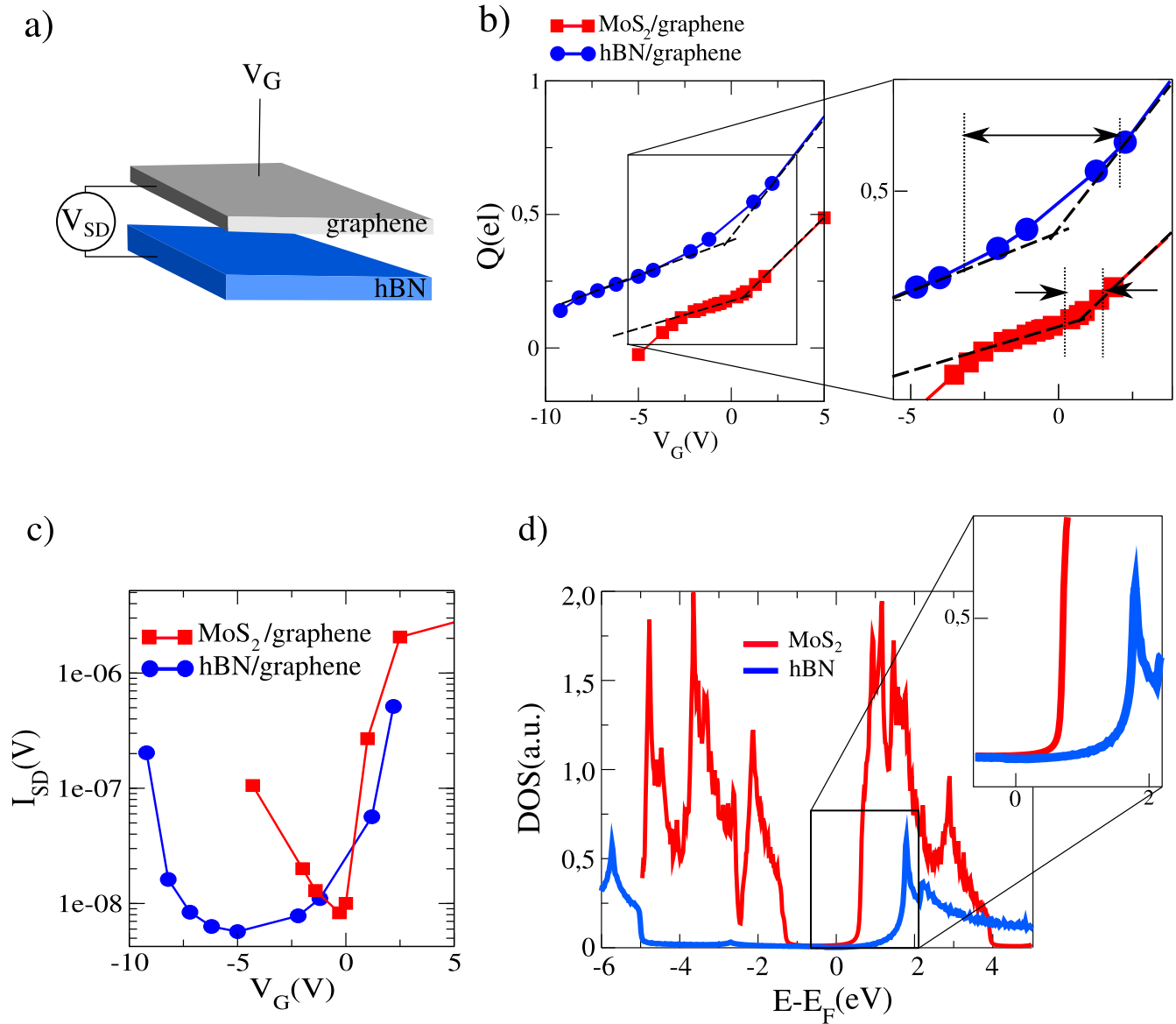


Figure 7. Graphic representation of the graphene/hBN interface is shown in (a). In (b) the charge transfer Q calculated on the graphene layer for hBN/graphene (blue line) is compared to the one calculated on graphene in graphene/MoS₂ (red line); the arrows on the right indicate the size of the switch region. In (c) the current calculated at the graphene/hBN interface as a function of V_G is indicated by the blue line, whereas the red line is the current corresponding to graphene/MoS₂, already shown in previous sections. In (d) the comparison is shown between the partial DOS of MoS₂ (red solid and dashed lines) and that of hBN (blue line). CB edges have a different shape, smoother in hBN than in MoS₂, as shown in the inset.

related to smoother CB edges of hBN (blue line in figure 7(d) around 1 and 2 eV) with respect to the one of MoS₂.

4. Independence of the interfaces in vdW heterostructures

In this brief section, we would like to show the possibility to predict the shape of the charge transfer Q on the intermediate layer in a mixed heterostructure, by considering separately the single interfaces and the charge transfer Q between them. Here, we consider the MoS₂/hBN/graphene heterostructure, which can be decomposed in two different interfaces, MoS₂/hBN and hBN/graphene, represented in figure 8(a).

Here, we just compare the sum of the charge transfer Q on graphene calculated in the separate interfaces, 2) + 3), 2) and 3) in figure 8(b) (the light and dark green for hBN-graphene and graphene-MoS₂, respectively), with Q on graphene calculated directly in the hBN/graphene/MoS₂ heterostructure (labeled 1) in figure 8(b).

Comparing the sum of Q from the separate interfaces and that calculated in the hBN/graphene/MoS₂ heterostructure, 2) + 3) and 1) in figure 8(b), we find a good agreement in the shape of the curve, whereas we have a vertical shift of approximately 0.1 electrons. However, as we illustrated in the main text, the shape of Q , in particular, the switch region and the ratio between the slopes in the ON and OFF linear region, are the most important parameters to characterize the current

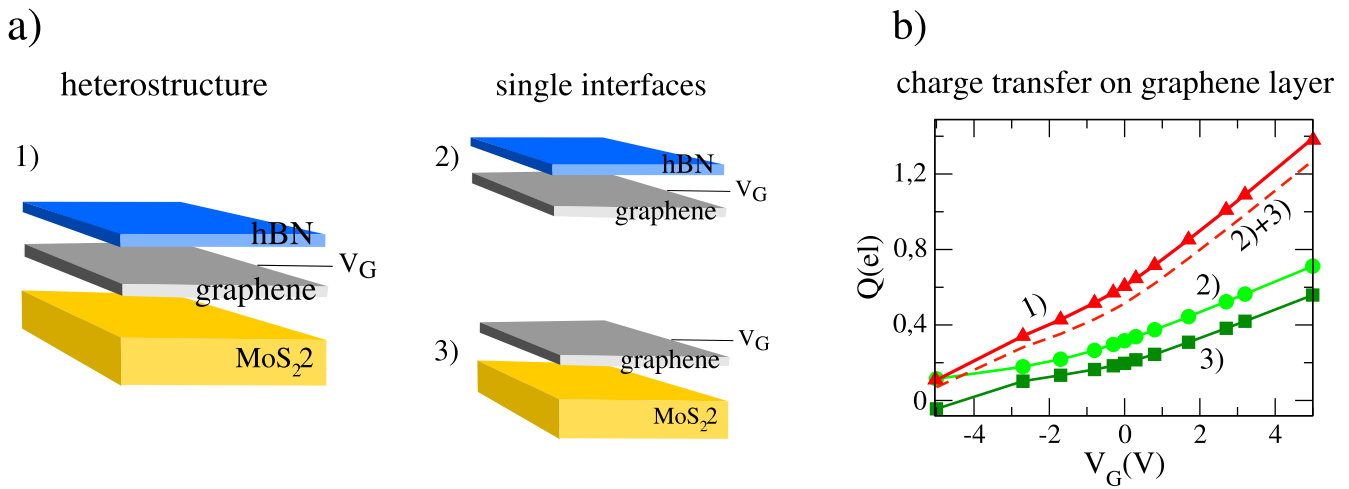


Figure 8. In (a) the hBN/graphene/MoS₂ heterostructure labeled 1). 2) and 3) are the graphic representations of the single interfaces of hBN/graphene and graphene/MoS₂. In (b) we plot the charge transfer Q on graphene, calculated directly in 1) (red line) and as a sum of the Q calculated on graphene in the 2) and 3) interfaces (light and dark line, respectively). Dashed red line is Q calculated as a sum of the charge transfer in the single interfaces 2) and 3).

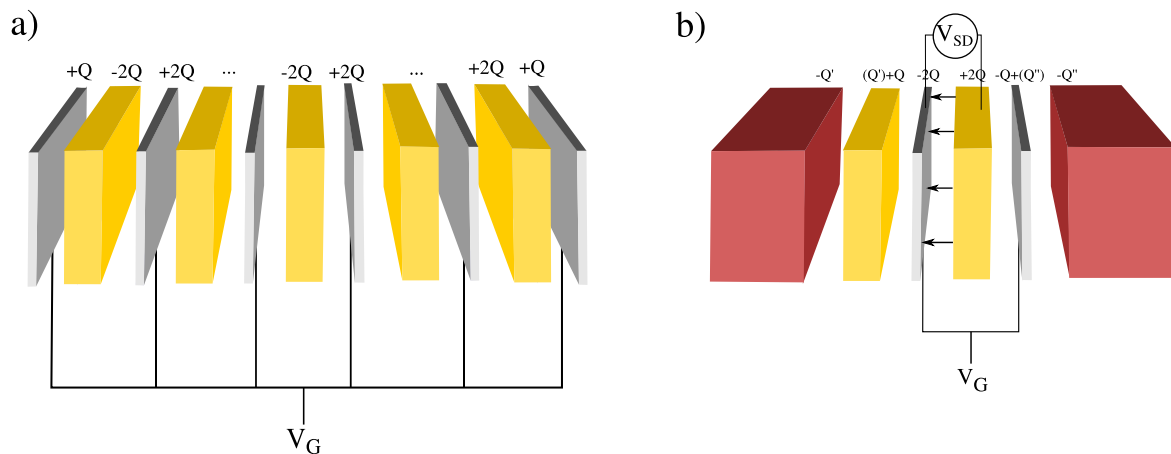


Figure 9. In (a) a sequence of alternate graphene-MoS₂ interfaces is represented, with graphene layers connected to a gate voltage; the charge transfer between the layers is given by a succession of $+2Q$ and $-2Q$. This demonstrates that the charge transfer on the layers in the middle is affected just by the closer plane and the presence of the farther layers is negligible. In (b) a scheme of the smallest heterostructure (MoS₂/graphene/MoS₂/graphene) that can be used to avoid the effect of the undesired charge transfer given by external layers (the red objects) on the electrodes is given, in this representation, by the graphene and MoS₂ in the middle.

at the interface. From a computational point of view, the possibility to succeed in this kind of prevision separating the single interfaces, is important because it avoids the problem related to the building of the supercell considering the mismatch between three or more different 2D crystals.

Furthermore, another interesting application of the independence of the interfaces is illustrated in this last part. Here, we report a simple scheme of a heterostructure composed of alternate graphene and MoS₂ planes beyond graphene/MoS₂/graphene/MoS₂. We found that the presence of the further planes does not change the charge transfer on the graphene-MoS₂ interface in the middle (see figure 9(a)).

This kind of independence found in the vdW heterostructure interfaces when the alternate graphene layers are connected to the gate, can be useful if one wants to avoid the charge dispersion on the electrodes. One possible structure is represented in figure 9(b): if we add extra vdW layers on the top and bottom

of MoS₂/graphene/MoS₂/graphene, as the capper in the transistor, for instance, the charge transfer necessarily present at the external interfaces does not affect the charge transfer and consequently the electronic transport between the electrodes.

5. Conclusions

In conclusion, in this work we have studied the mechanism at the basis of the graphene/MoS₂ transistor performance by observing and comparing the results coming from three heterostructures of alternate graphene and MoS₂ layers. In all these systems, we have chosen the graphene and MoS₂ electrodes where the electronic transport calculations were performed, and we have studied the influence of the additional layers on the performance of the transistors. We have focused our attention on the current modulation as a function

of the gate voltage, namely $I_{SD}(V_G)$, relating its behavior to the charge transfer Q (and, consequently, to the band shift). We found that the width of the switch region is strictly related to the slope of $I_{SD}(V_G)$. The faster the change of slope of the charge transfer from the OFF to ON region occurs, namely for small V_G range, the more $I_{SD}(V_G)$ will rapidly increase.

By stacking additional layers, it is possible to tune the effect of the gate voltage on the band shift and, consequently, on the charge transfer. We have seen that one is able to reduce the effect of V_G on the charge transfer and on the current just by adding an extra graphene layer non-connected to the gate as in the first graphene/MoS₂/graphene, worsening the performance of the transistor. On the other hand, we can improve the V_G effect on the charge transfer on the electrodes, connecting also the second graphene to the gate potential. However, even if Q is doubled on the electrodes, the current does not switch faster, since neither the *velocity* of the Q curve moving from the OFF to the ON region, nor the increased ratio of Q , namely the ratio between the ON and OFF region slope, change. By stacking additional layers, the current can at least show an increase in the ON/OFF ratio, probably due to more charges at the Fermi level, determining the current.

We found that the heterostructures composed of alternate layers beyond the electrodes do not represent the way to really improve the transistor performance. Moreover, further additional planes beyond MoS₂/graphene/MoS₂/graphene do not affect even the charge transfer on the electrodes, as a consequence of the interface independence. However, this kind of independence found in the vdW heterostructure interfaces when the alternate graphene layers are connected to the gate, can be useful if we want to avoid the charge dispersion on the electrodes. If an extra vdW layers is on the top and bottom of the MoS₂/graphene/MoS₂/graphene, as the capper in the transistor, for instance, the necessary charge transfer present at the external interfaces does not affect the charge transfer and consequently the electronic transport between the electrodes.

Moreover, the independence of the interfaces can also be used to study the heterostructures composed of more than two different crystals such as, for example, hBN/graphene/MoS₂. The possibility to separate the two interfaces allows us to avoid the computational problem of the lattice mismatch between three crystals and to build and analyze even different supercells with a different size for each interface. For example, it is possible to study, within the framework of DFT, transistors with a more complex structure, made by vertical stacking of 2D crystals, just by considering separately each interface.

We can conclude by saying that the mixed vertical heterostructures composed of more than two different crystals are not useful to improve the performance of the transistor, whereas the choice of the semiconductor with a sharp band edge is more important to increase the current slope for a fast switching device.

Acknowledgments

D Di Felice thanks the CEA Phare Program for funding her research.

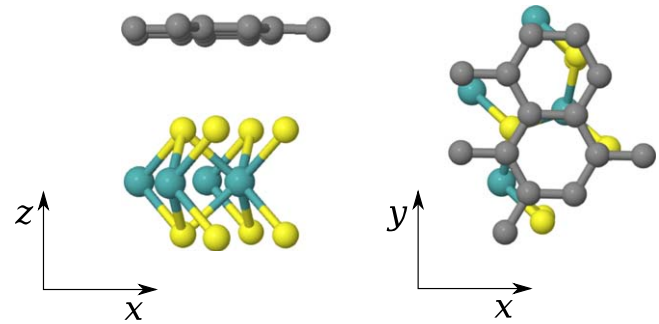


Figure A1. Representation of the basic graphene/MoS₂ cell used in our calculations.

Appendix A. Unit cell optimization

The unit cell we used to build the four configurations is composed of graphene/MoS₂ mutually rotated 15 degrees, see figure A1. All the other configurations are built by adding one graphene layer, one MoS₂ or both in a vertical stacking.

Following the Fireball formalism based on the self-consistent Harris–Foulkes LDA functional, the structural optimization is performed until the forces were below 0.1 eV/Å. Optimized numerical basis sets have been used for molybdenum (Mo), sulfur (S) and carbon (C) with respective cutoff radii in atomic units of $s = 3.9$, $p = 4.5$, $d = 5.0$ for S, $s = 5.0$, $p = 4.5$, $d = 4.8$ for Mo and $s = 4.5$, $p = 4.5$ for C. The choice of the supercells is a well-known problem in DFT codes as already dealt with in our previous article [31] with respect to the effect of the rotation angle on the electronic properties of graphene/MoS₂ heterostructure. Hence, due to the lattice vector mismatch and rotation angle, a perfect match is very difficult to obtain. Consequently, it is necessary to adapt the lattice vector parameter of graphene and MoS₂ by applying an artificial strain on the two layers that can affect the electronic properties. In our previous article, we found a way to treat this problem by studying the effect of the strain on the electronic properties of graphene and MoS₂. We found that the MoS₂ electronic gap is very sensitive to the strain, whereas on graphene electronic structure the effect of the strain is negligible. Consequently, we chose to keep the MoS₂ layer in the optimized structure, while graphene presents a small strain. Furthermore, while LDA functional is a good approximation for covalent bonds characterizing the in-plane interactions, the out-of-plane vdW interactions are not well dealt with in DFT. This well-known limit of DFT in dealing with the vdW interaction, is overcome by using the LCAO-S² + vdW approach [32], based on the dipolar approximation for vdW interaction. This approach has proved to give good results in agreement with experiments [33–35]. The structural optimization is thus performed in two steps: a preliminary equilibrium configuration is obtained by using LDA functional, and then the LCAO-S² + vdW approach is used to calculate the equilibrium interlayer distance, found to be ~ 3.1 Å, as reported in [31].

Appendix B. The scissor operator

The scissor operator consists of an extra potential added to the sub-Hamiltonian written in the localized orbital basis set of a system, in order to shift the electronic levels of the corresponding subsystem with respect to the rest of the system. It can be seen as an extra electric field applied to one subsystem. In the present case, we shift the electronic levels of the graphene monolayer with respect to the levels of MoS₂, in order to reproduce the effect of an electrostatic gate applied to the system. Since this operator is part of the Hamiltonian, the electronic density is correctly recalculated through the usual self-consistent process, and the charge transfer is correctly taken into account. This approximation works very well here due to the weak coupling between the 2D materials through vdW interaction. This method has been developed first for metal/organic interfaces to correct the electronic level misalignment [36]. It has then been generalized to extended interfaces in our previous work [31].

The scissor operator, in the most general case, is able to move each band $\varepsilon_\alpha(\mathbf{k})$ a value $\Delta_\alpha(\mathbf{k})$. Taking advantage of the properties of projectors, it can be written as:

$$O^S = \sum_{\alpha, \mathbf{k}} \Delta_\alpha(\mathbf{k}) |\alpha(\mathbf{k})\rangle \langle \alpha(\mathbf{k})|, \quad (2)$$

where $|\alpha(\mathbf{k})\rangle$ is the eigenorbital with energy $\varepsilon_\alpha(\mathbf{k})$. We will calculate the matrix elements of the scissor operator in the Fireball basis set for periodic systems:

$$|B_{\mu,i}(\mathbf{k})\rangle = \frac{1}{\sqrt{N}} \sum_{\mathbf{R}} e^{i\mathbf{k}(\mathbf{R}+r_i)} |\phi_{\mu,i}\rangle, \quad (3)$$

where $|\phi_{\mu,i}\rangle$ is the numeric atomic orbital of the orbital μ of atom i (at r_i). If we expand $|\alpha(\mathbf{k})\rangle$ in this basis set:

$$|\alpha(\mathbf{k})\rangle = \sum_{\lambda,l} b_{\lambda,l}^\alpha(\mathbf{R}) |B_{\lambda,l}(\mathbf{k})\rangle, \quad (4)$$

the scissor operator matrix element $\langle B_{\mu,i}(\mathbf{k}) | O^S | B_{\nu,j}(\mathbf{k}) \rangle$ takes the form:

$$\langle B_{\mu,i}(\mathbf{k}) | O^S | B_{\nu,j}(\mathbf{k}) \rangle = \sum_{\alpha} \Delta_\alpha(\mathbf{k}) \langle B_{\mu,i}(\mathbf{k}) | \left(\sum_{\lambda,l} b_{\lambda,l}^\alpha(\mathbf{R}) |B_{\lambda,l}(\mathbf{k})\rangle \right) \times, \quad (5)$$

$$\times \left(\sum_{\sigma,m} b_{\sigma,m}^{\alpha,*}(\mathbf{R}) \langle B_{\sigma,m}(\mathbf{k}) | \right) | B_{\nu,j}(\mathbf{k}) \rangle =, \quad (6)$$

$$\sum_{\alpha,l,m,\lambda,\sigma} \Delta_\alpha(\mathbf{k}) b_{\lambda,l}^\alpha(\mathbf{R}) b_{\sigma,m}^{\alpha,*}(\mathbf{R}) \underbrace{\langle B_{\mu,i}(\mathbf{k}) | B_{\lambda,l}(\mathbf{k}) \rangle}_{S_{\mu,i;\lambda,l}(\mathbf{k})} \times \underbrace{\langle B_{\sigma,m}(\mathbf{k}) | B_{\nu,j}(\mathbf{k}) \rangle}_{S_{\sigma,m;\nu,j}(\mathbf{k})}, \quad (7)$$

where $S_{\mu,i;\lambda,l}(\mathbf{k})$ is the overlap matrix element between the orbital μ of atom i and the orbital λ of atom l .

In our calculations, the scissor operator has been applied only on graphene, by selecting the eigenorbitals $|\alpha(\mathbf{k})\rangle$ corresponding to carbon atoms. The initial shift given by $\Delta_\alpha(\mathbf{k})$ is applied on the selected eigenorbitals (all the carbon

orbitals), which build the graphene sub-Hamiltonian. This sub-Hamiltonian is part of the whole Hamiltonian over which the self-consistency is performed. Thus, the whole system reacts to the scissor and the whole electronic density is recalculated. In our specific case, when the self-consistency is reached, the energy shift of the graphene eigenvalues with respect to MoS₂ is always lower than the applied $\Delta_\alpha(\mathbf{k})$, as a consequence of the response of the system. In this work, we refer to the gate voltage as the value of $\Delta_\alpha(\mathbf{k})$ applied on the graphene eigenorbitals. Thus, V_G and $\Delta_\alpha(\mathbf{k})$ have the same value. Moreover, the value of $\Delta_\alpha(\mathbf{k})$ is the same for all the eigenorbitals where it is applied.

ORCID iDs

Y J Dappe  <https://orcid.org/0000-0002-1358-3474>

References

- [1] Schwierz F *et al* 2015 *Nanoscale* **7** 8261
- [2] Moore G E 1965 *Electronics* **38** 114–77
- [3] Dennard R H *et al* 1974 *IEEE J. Solid-State Circuits* **9** 256–68
- [4] Mistry K *et al* 2007 *IEEE International Electron Devices Meeting (Washington, DC, 10–12 December 2007)* 247–50
- [5] Cartwright J 2011 *Nature* **38** 114–77
- [6] Ferrain I *et al* 2011 *Nature* **479** 310–6
- [7] Colinge J P 2004 *Solid State Electron* **48** 897–905
- [8] Novoselov K S *et al* 2004 *Science* **306** 666
- [9] Novoselov K S *et al* 2012 *Nature* **490** 192
- [10] Geim A K and Grigorieva I V 2013 *Nature* **499** 419
- [11] Radisavljevic B *et al* 2011 *Nature* **6** 147
- [12] Yoon Y *et al* 2011 *Nano Lett.* **11** 3768–73
- [13] Myoung N *et al* 2013 *ACS Nano* **7** 7021–7
- [14] Britnell L *et al* 2012 *Science* **335** 947
- [15] Yu W J *et al* 2013 *Nat. Mater.* **12** 246
- [16] Singh A K *et al* 2016 *ACS Appl. Mater. Interfaces* **8** 34699–705
- [17] Luryi S 1988 *Appl. Phys. Lett.* **52** 201
- [18] Heiblum M *et al* 1990 *IBM J. Res. Develop.* **34** 530
- [19] Simmons J A *et al* 1998 *J. Appl. Phys.* **84** 5626
- [20] Zaslavsky A *et al* 2003 *Appl. Phys. Lett.* **83** 1653
- [21] Sciambi A *et al* 2011 *Phys. Rev. B* **84** 085301
- [22] Roy T *et al* 2014 *ACS Nano* **8** 6259–64
- [23] Lewis J P *et al* 2011 *Phys. Status Solidi B* **248** 1989
- [24] Jelínek P *et al* 2005 *Phys. Rev. B* **71** 235101
- [25] Harris J 1985 *Phys. Rev. B* **31** 1770–9
- [26] Foulkes W M C and Haydock R 1989 *Phys. Rev. B* **39** 12520–36
- [27] Keldysh L V 1964 *Zh. Eksp. Teor. Fiz* **47** 1515
Keldysh L V 1965 *Sov. Phys. JEPT* **20** 1018
Mingo N *et al* 1996 *Phys. Rev. B* **54** 2225
- [28] Gonzalez C *et al* 2016 *Nanotechnology* **27** 105702
- [29] Abad E *et al* 2010 *J. Phys.: Condens. Matter* **30** 04007
- [30] Abad E 2013 *Energy Level Alignment and Electron Transport Through Metal/Organic Contacts* (Heidelberg: Springer)
- [31] Di Felice D *et al* 2017 *J. Phys. D: Appl. Phys.* **50** 17LT02
- [32] Dappe Y J *et al* 2006 *Phys. Rev. B* **74** 205434
- [33] Dau M T *et al* 2018 *ACS Nano* **12** 2319
- [34] Pierucci D *et al* 2016 *Sci. Rep.* **6** 26656
- [35] Savini G *et al* 2011 *Carbon* **49** 62
- [36] Abad E *et al* 2011 *J. Chem. Phys.* **134** 044701